Guetta-Terrier et al., http://www.jcb.org/cgi/content/full/jcb.201501106/DC1

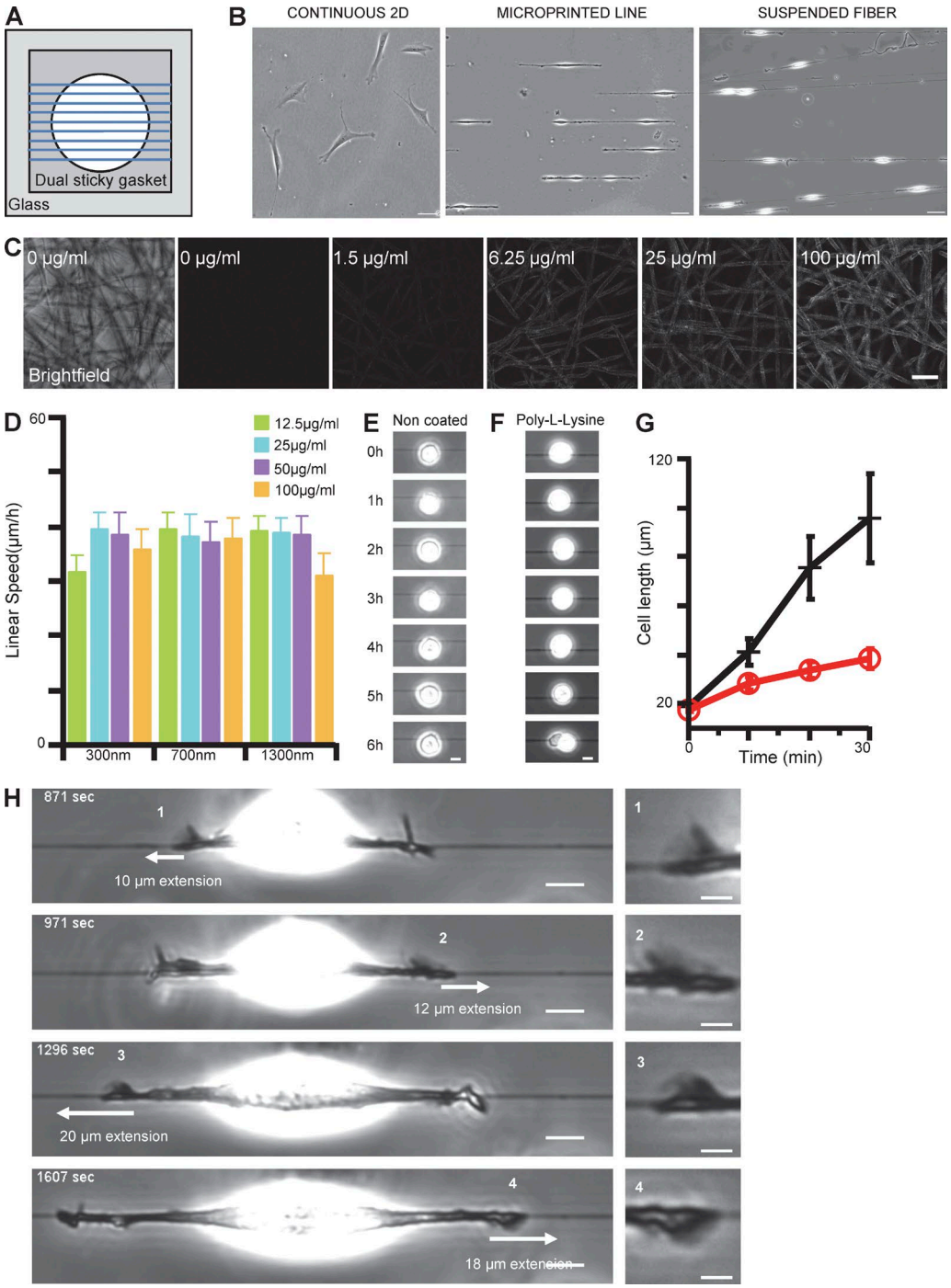

Figure S1. **Experimental system and complementary results on cell speed and spreading.** (A) Drawing of the system: a double-sided sticky gasket is used to suspend fiber on a closed-microchamber. (B) Snapshots of 3T3 cell on continuous surface (left), microprinted line (middle), and suspended fiber (right). Bar, 50 µm. (C) Meshwork of fibers coated with a serial concentration of fluorescent fibronectin. The higher the concentration of fluorescent fibronectin, the higher the intensity. (D) Quantification of the linear speed of cells plated on fibers with different concentrations of fibronectin (12.5, 25, 50, and 100 µg/ml) and diameters (300 nm, 700 nm, and 1.3 µm). Error bars, SEM; NB, from left to right, 56, 92, 25, 24, 63, 47, 65, 40, 126, 67, 59, 27. (E and F) Influence of the coating: 3T3 cells were plated on uncoated fiber (E) and poly-L-lysine (F) and imaged for 6 h. Bars, 10 µm. (G) Spreading kinetics of control cells (black line) compared with Arp2/3 inhibited cells (red line) plated on fiber. Error bars, SEM; NB, 7 (control), 10 (CK666). (H) Time sequence of 3T3 fibroblast spreading on fiber. For each time point we identified a fin-like protrusion responsible for leading edge extension. White arrows, amount of extension for each fin; their length is proportional of leading edge advancement. The square images on the right are zooms of fins. Bar, 10 µm.

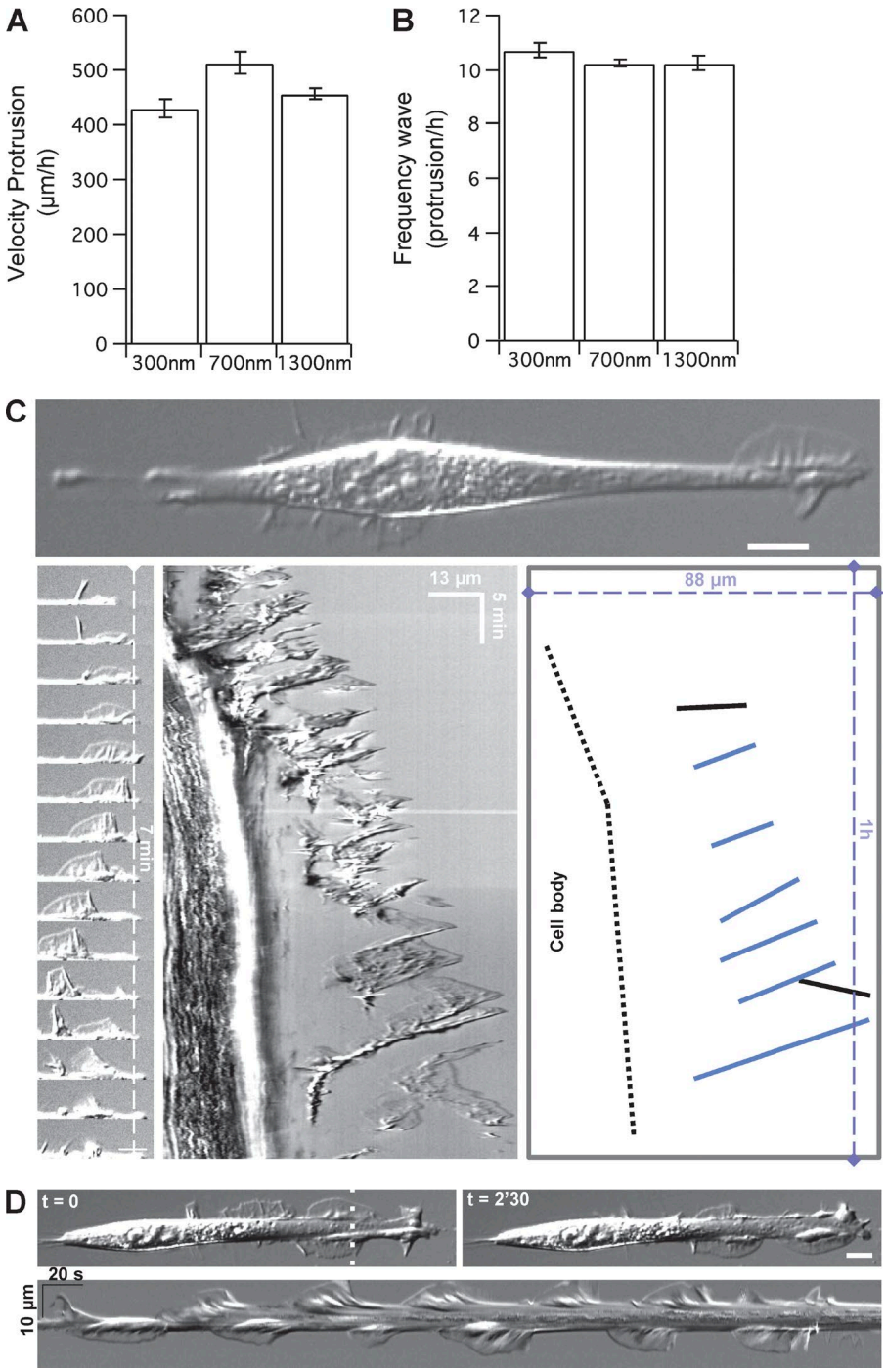

Figure S2. **Analysis of cell behavior on fibers of different diameters and on printed lines.** (A) Quantification of the velocity of the protrusion depending on the fiber diameter. (Error bars, SEM; NB, from left to right, 45, 25, and 56). (B) Quantification of the frequency of the protrusion depending on the fiber diameter. NB, from left to right, 11, 9, and 11. (C) 3T3 fibroblast on a microprinted line (top panel). Bar, 10 µm. Protrusion was formed preferentially radial to the line. Zoom of the formation of protrusion on microprinted line (bottom left panel). Kymograph of the propagation of protrusions along the line (bottom middle panel). Schematic analysis of the kymograph (bottom right panel). (D) Cell displays radial protrusion on the line: protrusions beyond the line can alternate from top to bottom (top). Bar, 10 µm. Kymographs radial to the line showing robust lamellipodia alternations between opposite cell sides (bottom).

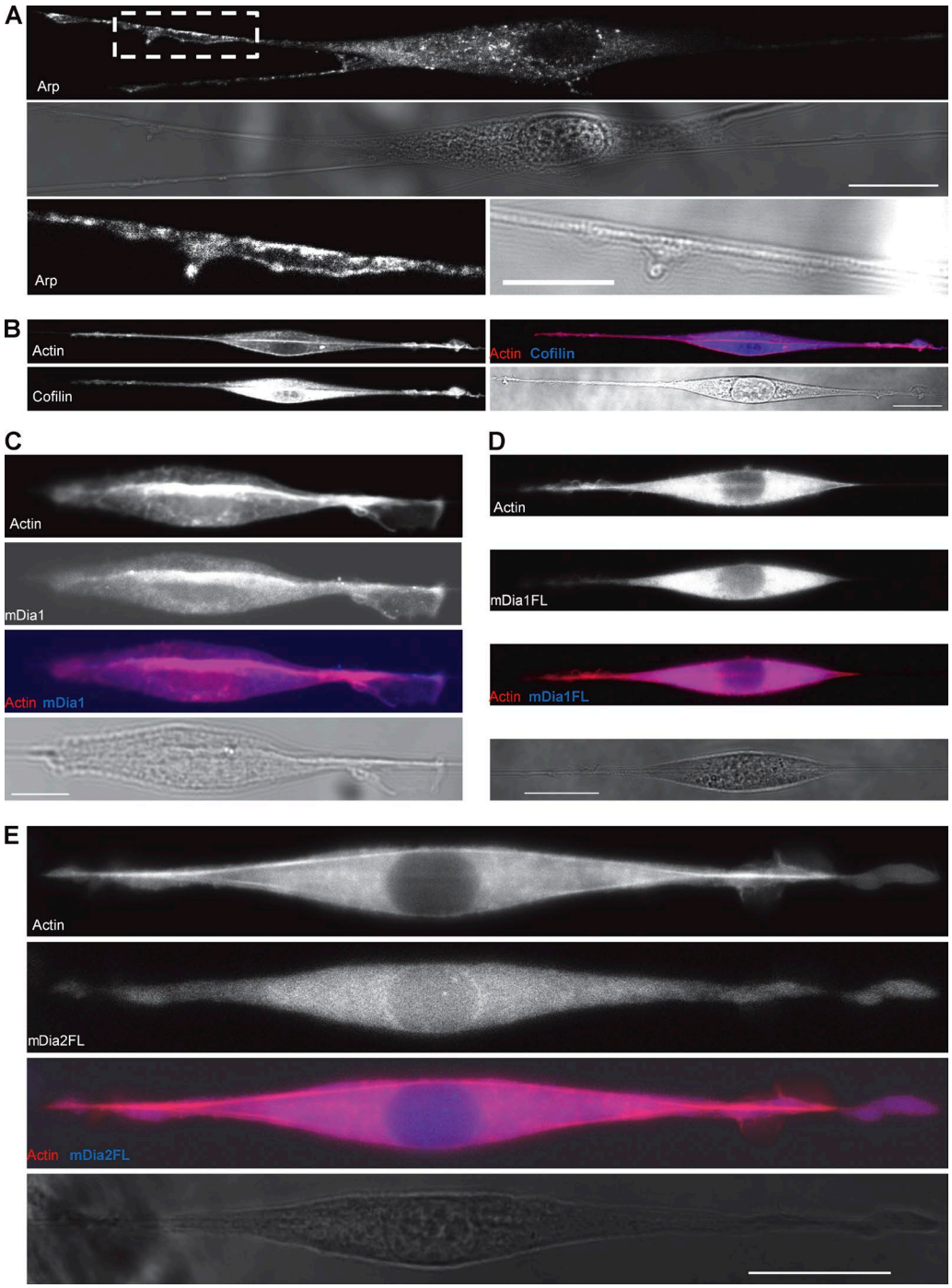

Figure S3. **Fluorescent staining for different actin-polimerizing machineries.** 3T3 cells on fibers were fixed and stained for (A) anti-Arp3 (bar, 20 µm [top two panels], 10 µm [bottom panels], (B) anti-Cofilin and actin phalloidin (bar, 20 µm), (C) anti-mDia1 and actin phalloidin (bar, 10 µm), (D) 3T3 cell transfected with GFP-mDia1 full length and RFP-actin and plated on fiber (bar, 20 µm), and (E) 3T3 cell transfected with GFP-mDia2 full length and RFP-actin and plated on fiber (bar, 20 µm).

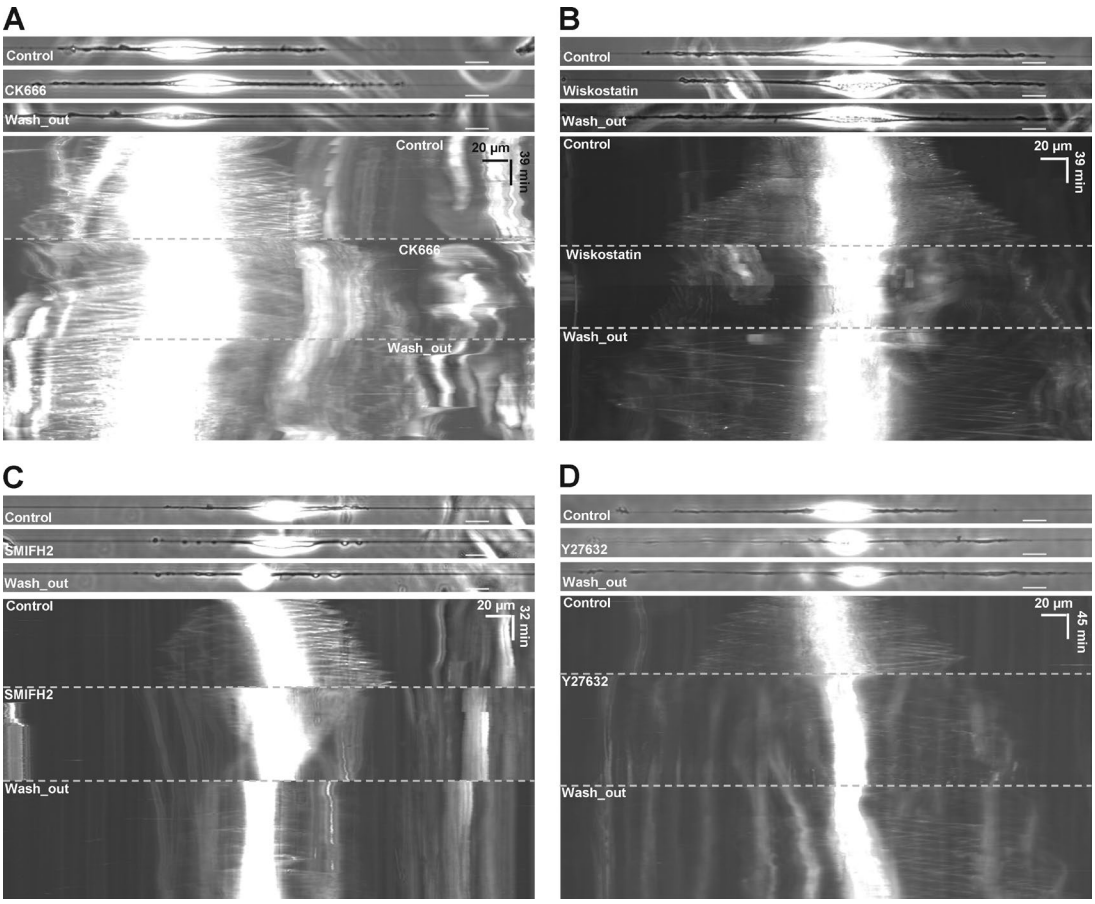

Figure S4. **Kymographs of washout experiments for 3T3 cells seeded on fiber.** (A) CK666, (B) wiskostatin, (C) SMIFH2, and (D) Y27632. Bar, 20 µm.

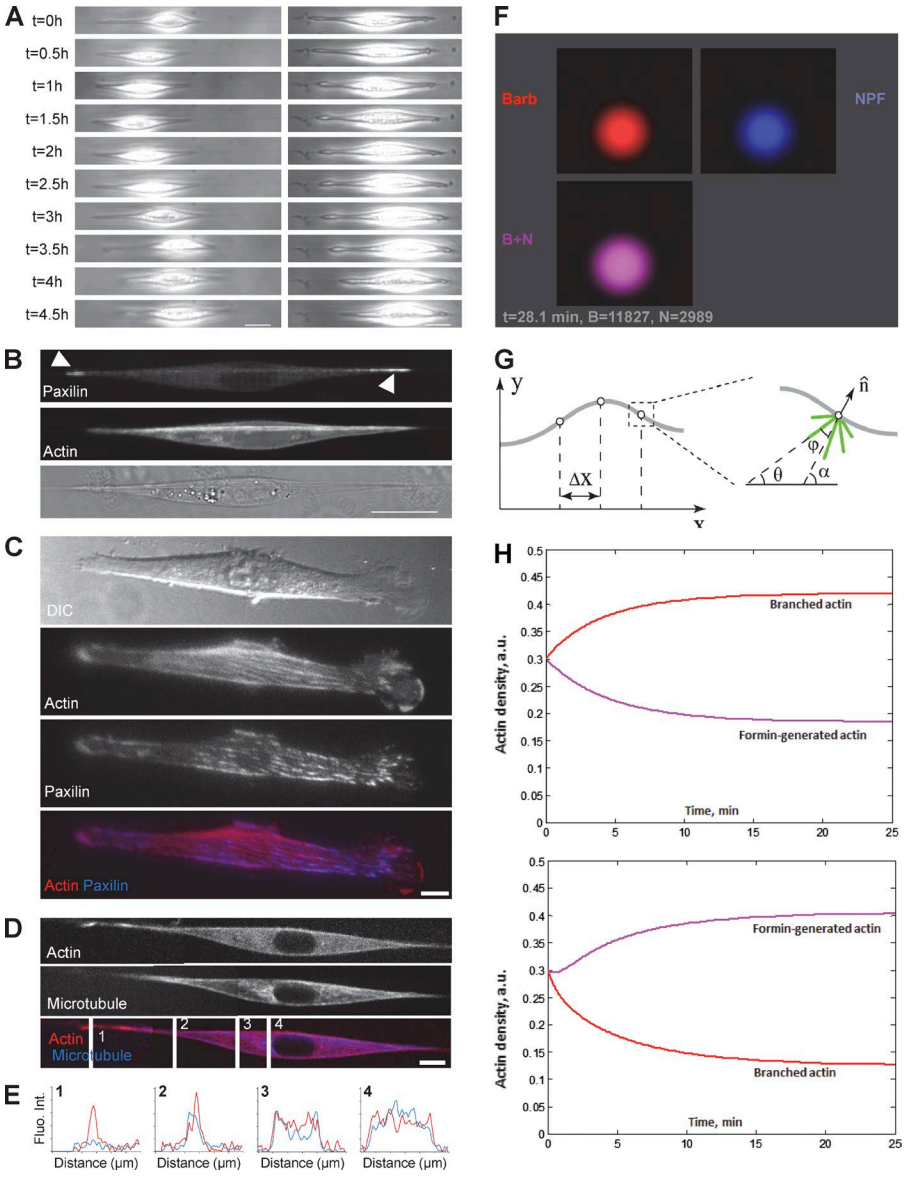

Figure S5. **Complementary experiments with MDCK cells on fiber and 3T3 cells on line and fiber as well as figures from the mathematical modeling.** (A) Snapshots of MDCK cell over 4.5 h (1 frame/0.5 h) on suspended fiber. Bar, 20 μm. MDCK did not display fin-like protrusions. (B) MDCK cells were fixed and stained for anti-Paxilin and actin phalloidin. Bar, 20 μm. (C) 3T3 cells were transfected with GFP-Actin and RFP-Paxilin and seeded on microprinted line and observed using total internal reflection microscopy. Mature focal adhesions were formed along the line. Bar, 10 μm. (D and E) 3T3 cells were transfected with GFP-Tubulin and RFP-Actin and plated on fiber. (D) Microtubules were not colocalized with actin at the end of the protrusion but colocalized at the end of the spindle-shaped cell body. Bar, 10 μm. (E) Quantification of the intensity of fluorescent tubulin at different regions: end of protrusion (1), end of cell body (2), middle of the spindle shape (3), and near the nucleus (4) for one typical cell. In the cell body, as opposed to actin, microtubules were cortical and localized near the Golgi apparatus. (F) Predicted stationary distributions of the barbed ends and NPFs. The barbed end density is shown in red; the NPF density is shown in blue; combined density is shown in purple. (G) Schematic of the model. Gray lines, leading edge; circles, membrane nodes; green lines, actin filament arrays growing at angle θ relative to the baseline; α is the angle of the local vector normal to the leading edge; ϕ is the angle between the orientation of the actin array and the direction locally normal to the leading edge. (H) Predicted densities of the branched and formin-generated F-actin networks in the model with competition for G-actin. Branched actin and formin-generated actin densities are shown in red and purple, respectively. The time series for two densities are shown when the growth rate for branched network is greater (left: $\tilde{k}_1$ = 1.2/[unit × min]) and smaller (right: $\tilde{k}_1$ = 0.8/[unit × min]) than the growth rate for formin-generated network $\tilde{k}_8$ = 1/(unit × min).

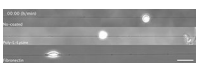

Video 1. **Comparison of 3T3 behavior in different coating of fiber.** 3T3 fibroblasts were plated on uncoated fiber, poly-L-lysine–coated fiber and fibronectin-coated fiber. Cells were imaged in phase contrast with a 10× objective (IX81; Olympus) for 12 h (one image every 2 min). Bar, 50 μm.

Video 2. **Comparison of migration behavior on different substrates.** 3T3 cells were plated on continuous surface, microprinted line, and suspended fiber coated with fibronectin. Cells were imaged in phase contrast with a 10× objective (IX81; Olympus) for 6 h and cell bodies were manually tracked one image every 10 min (red, green, and blue lines for the tracks on continuous surface, microprinted line, and suspended fiber). Bar, 10 µm.

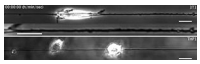

Video 3. **3T3 migration on suspended fiber, formation of fin-like protrusion versus TPH1 on suspended fiber, and no fin-like protrusion.** 3T3 fibroblast was plated on fibronectin-coated fiber. Cell was imaged in phase contrast with a 20× objective (IX81; Olympus), one image every 30 s for 108 min. Cell displayed fin-like protrusion. Bar, 20 µm (top and middle). TPH1 cells were plated on fibronectin-coated fiber. Cells were imaged in phase contrast with a 20× objective (IX81; Olympus), one image every 30 s for 108 min. This cell type did not display fin-like protrusion. Bar, 20 µm (bottom).

Video 4. **3T3 migration on microprinted-line.** 3T3 fibroblasts were plated on microprinted line coated with fibronectin. Cells were imaged in DIC with a 20× objective (IX81; Olympus), one image every 2 s for 1 h 3 min 48 s. Cells preferentially extended protrusions beyond the line. Bar, 10 µm.

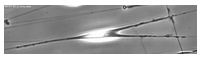

Video 5. **Fin-like protrusion in a cell spanning between multiple fibers.** Concatenation of five movies showing 3T3 cells, plated on fibers, and imaged in phase contrast (IX81; Olympus; 20× or 10× objective), one image every 30 s (A for 9 min 30 s and B for 3 h 30 min) and one image every 2 min (C for 8 h 58 min, D for 10 h 16 min, and F for 8 h 18 min). Bar, 20 µm.

Video 6. **3T3 migration on suspended fiber: correlation between fin and polarization.** Concatenation of 10 movies showing 3T3 cells plated on fibronectin-coated fiber. Cells were imaged in phase contrast (IX81; Olympus; 20× or 10× objective), one image every 30 s (A, B, E, and G for 6 h; C for 4 h 32 min; D for 4 h 44 min; and F for 4 h 33 min) or one image every 2 min (H for 8 h 34 min, I for 11 h 26 min, and I for 12h). Fin-like protrusions were correlated with cell polarity. Bar, 20 µm.

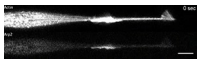

Video 7. **Arp2/3-mediated cell polarization.** 3T3 cells were transfected with GFP-Actin and mCherry-Arp2 and plated on single suspended fiber. Cell was imaged with 63× objective (confocal microscopy; Carl Zeiss), one image every 5 s for 195 s (top: actin; bottom: Arp2). Bar, 10 µm.

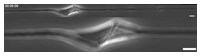

Video 8. **Force application and matric deformation on fiber.** 3T3 cell plated on fibronectin-coated fiber was able to deform its environment by pulling and coiling the fiber. It is worth noticing that the fin formation occurred only on the pulling side: on the left side of the cell during the first 30 min; on the right side from 30 min to 2 h; on both sides from 2 h to the end, when the force was equilibrated. Cell was imaged in phase contrast with a 20× objective (IX81; Olympus), one image every 30 s for 3 h 21 min. Bar, 10 µm.

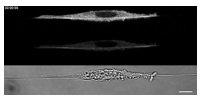

Video 9. **An alternative mode of protrusion.** 3T3 cells were transfected with GFP-Talin and RFP-Paxilin. A clear lack of persistence was observed with the cell changing direction. The change of cell polarity (four times) was accompanied by polarity shift for lobopodia and blebs (from the left to the right or from the right to the left, respectively). Cell was imaged with 63× objective (confocal microscopy; Carl Zeiss), one image every 10 s for 2 h 2 min 10 s. Bar, 10 µm.

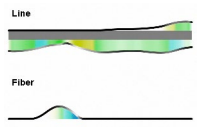

Video 10. **Simulation of protrusion dynamics on line and fiber.** On line (top), protrusions were waving, spreading, and collapsing intermittently, in a fashion similar to the observed unstable lamellipodia. On fiber (bottom), protrusions were forming fin-shaped structures that were stable and propagating along the fiber, in a fashion similar to the observed phenotype in cells.

Table S1. **Appearance of fin-like protrusions in different cell types**

Categories	Name	Type	Fin
Fibroblast	3T3	Mouse embryonic	+
	RPTP	Mouse embryonic	+
	REF	Rat embryonic	+
	Heart fibroblast	Neo rat cardiac	+
Epithelial	A341	Human	+
	HeLa	Human uterus	+
	HEK-293	Human embryonic	+
	MDCK	Canine kidney	–
Neurons-Brain like	C6	Rat glioma	+
	PC12	Rat neural crest	+
	NSC34	Mouse motor neuron	+
Immune	THP1	Macrophage-like (monocyte)	–
Endothelial	HUVEC	Human umbilical vein	+

Table S2. **Parameters for electrospinning of PCL fibers**

Variable	300 nm	700 nm	1,300 nm
Concentration (wt%)	12	12	12
Solvent	TFE/PBS = 1:4	TFE	TFE
Needle	22G	30G	30G
Flowing rate (ml/h)	0.7	0.5	1
Voltage (kV)	15	7	10
Distance (cm)	15	12	12

TFE, tetrafluoroethylene.